Original Article

http://dx.doi.org/10.4070/kcj.2016.46.1.63
Print ISSN 1738-5520 • On-line ISSN 1738-5555

kcj
Korean Circulation Journal

Genetic Variation of *SCN5A* in Korean Patients with Sick Sinus Syndrome

Young Soo Lee, MD[1*], Michael A Olaopa, PhD[2*], Byung Chun Jung, MD[3], Sang Hee Lee, MD[4], Dong Gu Shin, MD[4], Hyoung Seob Park, MD[5], Yongkeun Cho, MD[6], Sang Mi Han, MS[7], Myung Hoon Lee, PhD[7,8], and Yoon Nyun Kim, MD[5]

[1]*Division of Cardiology, Catholic University of Daegu, Daegu, Korea,* [2]*Krannert Institute of Cardiology, Indiana University School of Medicine, Indianapolis, IN, USA,* [3]*Daegu Fatima Hospital, Daegu,* [4]*Yeungnam University, Daegu,* [5]*Department of Internal Medicine, Keimyung University, Daegu,* [6]*Kyungpook National University, Daegu,* [7]*D&P Biotech, Daegu,* [8]*Department of Biochemistry and Cell Biology, Kyungpook National University, Daegu, Korea*

Background and Objectives: Due to recent studies that have shown an association between the genetic variation of *SCN5A* and sick sinus syndrome (SSS), we sought to determine if a similar correlation existed in Korean patients with SSS.

Subjects and Methods: We enrolled 30 patients with SSS who showed a sinus pause (longer than 3.0 s) in Holter monitoring, in addition to 80 controls. All exons including the putative splicing sites of the *SCN5A* gene were amplified by polymerase chain reaction and sequenced either directly or following subcloning. Wild-type and single nucleotide polymorphisms were expressed in human embryonic kidney cells, and the peak sodium current (I_{Na}) was analyzed using the whole-cell patch-clamp technique.

Results: A total of 9 genetic variations were identified: 7 variations (G87A-A29A, IVS9-3C>A, A1673G-H558R, G3823A-D1275N, T5457C-D1819D, T5963G-L1988R, and C5129T-S1710L) had been previously reported, and 2 variants (A3075T-E1025D and T4847A-F1616Y) were novel; the potential structural effects of F1616Y were analyzed in a three-dimensional model of the *SCN5A* domain. Patch-clamp studies at room temperature demonstrated that the peak I_{Na} was significantly increased by 140% in HEK cells transfected with F1616Y compared with wild-type (-335.13 pA/pF±24.04, n=8 vs. -139.95 pA/pF±23.76, n=7, respectively). Furthermore, the voltage dependency of the activation and steady-state inactivation of F1616Y were leftward-shifted compared with wild-type (V_h activation=-55.36 mv±0.22, n=8 vs. V_h activation=-44.21 mV±0.17, n=7; respectively; V_h inactivation=-104.47 mV±0.21, n=7 vs. V_h inactivation=-84.89 mV±0.09, n=12, respectively).

Conclusion: F1616Y may be associated with SSS. **(Korean Circ J 2016;46(1):63-71)**

KEY WORDS: *SCN5A* protein, human; Polymorphism, single nucleotide; Sick sinus syndrome.

Introduction

Conditions leading to sinus node dysfunction have considerable clinical importance. Sick sinus syndrome (SSS) manifesting as sinus bradycardia, sinus arrest, and/or sinoatrial block is the most frequent worldwide clinical indication for pacemaker implantation.[1)] Benson et al.[2)] screened *SCN5A* as a candidate gene in ten patients from families diagnosed with congenital SSS on the basis of disorders of cardiac rhythm and conduction during the first decade of life. Moreover, several investigations have linked variations in *SCN5A*, the gene encoding the pore-forming α-subunit of the cardiac-type sodium ion (Na^+) channel, Nav1.5, with familial SSS.[3-5)] Furthermore, the *SCN5A* gene is known to be associated with different forms of arrhythmias such as long QT syndrome, Brugada syndrome,

Received: February 20, 2015
Revision Received: May 18, 2015
Accepted: July 7, 2015
Correspondence: Yoon Nyun Kim, MD, Department of Internal Medicine, Keimyung University, 56 Dalseong-ro, Jung-gu, Daegu 41931, Korea
Tel: 82-53-250-7432, Fax: 82-53-250-7034
E-mail: ynkim@dsmc.or.kr

* These authors contributed equally to this work.

• The authors have no financial conflicts of interest.

Table 1. Multiplex polymerase chain reaction primers for amplification of the coding region of *SCN5A*

Exon #	Forward primers (5'→3')	Reverse primers (5'→3')
2	CTGGAGCCTCTCTGCAAATGGTGT	CCTCTTCCCCCTCTGCTCCATTGA
3	CTCTCCTCCTCCTCCCACCTCACC	GTCTTAGGACCAGCAGGGAATCAGC
4	CCCTGTTTATTGTCTGGTAGCACTGG	GTAAGTTCCTGGGCCTGGACACAAG
5	CCACGTAAGGAACCTGGAGAACCTG	GAAGCCAGAAAGAGAGGGGTGGTCT
6	CCCTGGGCTATCCACAGCACT	GTGGGGAAGACAGAGAGAGAGTCAC
7	AAGCCCAGGAGAAGCCTCCCTTATT	CTGTCTGGGTCTCTGGGGGATCAG
8	GGCACAGCCAGAGTTGCCTGAAG	CTCCAGAAGCTGTCTCCTCTGTGCT
9	TCACTGAGCTGTGGGGCATAAACTG	TGATCCCTTCTCCCTCAGAAGCAAG
10	CTTGGAAATGCCATAACCCAGAAGG	CCCCACCTATAGGCACCTACAGTCA
11	GGTGTGCAAGTCCACTTACTGATAGGG	GTGACTGTACAGGGGCCTAGCATGA
12	AGTTTAGCTGAGGCCAGTGGCACAA	CCAGCACACAGTAGGTGCTCAACAA
13	ACCTTCATCCTATCCCTGTGGCATC	GGGACAGTGTGGGGATGTCTAAAGC
14	TGTCACCTAGCAGCCCTGTCATCTC	GTGCAGGATCCCTTCTTCCTTACCC
15	CACAGCAAGAGTCAAGAGGCAGGTG	GTGATGACCTCAGATTGGGTTGTGC
16	GGAATAGGTGTCAGTGCCCTCCAAG	GGATGGACGGATGGGTAGATGGATT
17	GATTCAAGCCTCGGAGCTGTTTGTC	CCTTCTACCCCTACCCACTGCCAAG
18	AGATGCATGGGCAGGGTCTGAAAC	AAATGCAGGCATGCACCTCTCAC
19	GGAGCCCTAAGCTCCTGCAGACTC	TGGGCAGATATCTAAGGCAGGGTGT
20	CACCCCCATCATCGTAGCTCTTTCT	CTCTGCCCCAGTTTCTGACCTGACT
21	GGCAACAGAGCAAGACTGTCTCAAA	CTTCTCTTCCTCTGAGCCTGGGAAC
22	GAAGGCCTACTGTCTGTCCCCAACA	ATCAGAAGCACAGGGAGGGGTCCT
23	GCAGCCAGGGAGTTCATTCTTTCTT	CTTTGGGCACTGTGATCCTCCTATG
24	TGTCCAGACCAGAGCCCTAAGAAGC	AGATGCAGACACTGATTCCCTGGTG
25	CCACAGAATGGACACCCCTAGACAG	ATTCCAGCAGGAGCAAGAAGAGGAC
26	AGAGAAAGCCAGGAGGTGGTCAATC	CTCTACGAGGCTGGGACCTCTCTTC
27	GGGCTTTGGGCTCACTAGAGGGTAG	GGGTTGTACATGGCATTCAGCAGAG
28	CCTTGGCTCCTTGCCATATAGAGACC	GAGGCCCATTTCTTACTCCCAAAGC

progressive cardiac conduction defect, atrial fibrillation, dilated cardiomyopathy, and overlapping syndromes.[6)7)]

Voltage-gated Na^+ channels are transmembrane proteins that produce the fast inward Na^+ current responsible for the depolarization phase of the cardiac action potential. Inherited variations in *SCN5A* result in a spectrum of disease entities termed as Na^+ channelopathies.

To date, although many variations of the *SCN5A* gene have been documented in various cardiac diseases, *SCN5A* variations in Korean SSS patients have not yet been studied in detail. Therefore, we carried out complete sequencing of the coding regions of the *SCN5A* gene, excluding untranslated regions, in Korean SSS patients in order to identify any potential variations associated with SSS.

Subjects and Methods

Patient population

This study was approved by the Ethics Committee at each hospital; consent was obtained from all individuals before enrollment into the study. We enrolled 30 Korean patients with SSS and 80 controls with no cardiac symptoms. The diagnostic criterion for SSS was the presence of a pause longer than 3 seconds in the day-time during Holter monitoring or surface electrocardiography. Normal sinus function was confirmed in controls through a cardiac electrophysiological study after ablation for supraventricular tachycardia. We excluded the patients with atrial and ventricular arrhythmia such as atrial and ventricular tachycardia, atrial fibrillation and atrial flutter, atrioventricular block, Brugada syndrome, known malignancy, and a structurally abnormal heart.

Table 2. Baseline demographics of patients

No	Age	Gender	Height (cm)	Weight (kg)	DM	HTN	Symptom	LVEF (%)	Family history of SSS	Sinus pause (sec)
1	60	Male	164	88	Yes	Yes	Dizziness	58	No	3.3
2	57	Female	154	55	No	Yes	Dizziness	68	No	3.2
3	42	Male	172	73	No	Yes	Dizziness	64	No	3.4
4	47	Female	161	51	No	No	Syncope	57	No	6.1
5	60	Male	153	65	No	Yes	Syncope	68	No	6.0
6	44	Female	160	59	No	No	Dizziness	64	No	3.4
7	65	Female	153	59	No	No	Dizziness	68	No	3.7
8	58	Male	173	68	Yes	No	Dizziness	66	No	4.0
9	58	Female	162	57	No	No	Dizziness	71	No	3.7
10	65	Male	171	80	No	No	Syncope	57	No	8.4
11	57	Female	153	59	No	Yes	Syncope	67	No	6.3
12	58	Female	157	72	No	No	Dizziness	71	Yes	3.9
13	61	Female	171	77	Yes	No	Dizziness	64	No	3.4
14	58	Female	158	62	Yes	Yes	Syncope	76	No	6.2
15	65	Female	155	65	Yes	Yes	Dyspnea	77	No	4.3
16	27	Male	168	70	No	No	Dizziness	46	No	3.6
17	63	Female	154	64	No	Yes	Dyspnea	67	No	3.6
18	62	Female	146	63	Yes	Yes	Syncope	68	No	6.5
19	61	Female	148	59	Yes	No	Dizziness	57	No	4.8
20	39	Female	158	63	No	No	Dizziness	70	No	4.7
21	60	Female	147	58	No	No	Dizziness	75	No	4.2
22	59	Female	160	88	Yes	No	Dizziness	63	No	4.6
23	62	Male	167	74	No	No	Syncope	53	No	10.0
24	55	Female	157	61	No	No	Dizziness	71	No	3.1
25	52	Female	152	52	No	No	Syncope	71	No	5.8
26	59	Female	146	55	Yes	No	Dyspnea	59	No	3.2
27	45	Male	168	60	No	No	Dyspnea	60	No	4.2
28	59	Female	155	52	Yes	Yes	Syncope	52	No	5.6
29	64	Male	166	62	No	No	Dizziness	72	No	4.0
30	47	Female	155	51	No	No	Dizziness	64	No	4.6

DM: diabetes mellitus, HTN: hypertension, LVEF: left ventricular ejection fraction, SSS: sick sinus syndrome

Sampling and DNA extraction

All patient and control samples were recruited from the four participating medical centers: Keimyung University, Yeungnam University, Catholic University of Daegu, and Daegu Fatima Hospital. Peripheral bloods were collected in ethylenediamine tetraacetic acid (EDTA) containing tubes, and DNA was extracted from whole blood samples using the QIAamp DNA blood mini kit (Qiagen, Hilden, Germany). DNA concentration was determined using a NanoDrop ND1000 spectrophotometer, and the purity of the DNA was assessed based on the 260/280 nm absorbance ratio.

Multiplex polymerase chain reaction and sequence analysis

The coding region (exon 2-exon 28) of *SCN5A* was amplified by multiplex polymerase chain reaction (PCR) using newly designed primers (Table 1). PCR conditions were as follows: after an initial denaturation at 95℃ for 15 min, denaturation at 94℃ for 30 sec, annealing at 68-70℃ for 30-60 sec, and extension at 72℃ for 60-90 sec were repeated for 30-35 cycles. Following multiplex PCR,

http://dx.doi.org/10.4070/kcj.2016.46.1.63

Table 3. Genetic variations in the *SCN5A* gene and their frequency in Korean patients with sick sinus syndrome (N=30) and normal controls (N=80)

dbSNP ID	Variation	N	Exon	Genotype frequency (N/%)		
	G87A (A29A)			GG	GA	AA
rs6599230	Case	30	2	11 (36.7)	15 (50.0)	4 (13.3)
	Control	80		36 (45.0)	36 (45.0)	8 (10.0)
	IVS9-3C>A			CC	CA	AA
rs41312433	Case	30	intron 9	22 (73.3)	8 (26.7)	0 (0.0)
	Control	80		61 (76.3)	19 (23.8)	0 (0.0)
	A1673G (H558R)			AA	AG	GG
rs1805124	Case	30	12	22 (73.3)	8 (26.7)	0 (0.0)
	Control	80		59 (73.8)	21 (26.3)	0 (0.0)
	A3075T (E1025D)			AA	AT	TT
	Case	30	17	29 (96.7)	1 (3.3)	0 (0.0)
	Control	80		80 (100.0)	0 (0.0)	0 (0.0)
	G3823A (D1275N)			GG	GA	AA
	Case	30	21	28 (93.3)	2 (6.7)	0 (0.0)
	Control	80		80 (100.0)	0 (0.0)	0 (0.0)
	T4847A (F1616Y)			TT	TA	AA
	Case	30	28	29 (96.7)	1 (3.3)	0 (0.0)
	Control	80		80 (100.0)	0 (0.0)	0 (0.0)
	C5129T (S1710L)			CC	CT	TT
	Case	30	28	29 (96.7)	1 (3.3)	0 (0.0)
	Control	80		80 (100.0)	0 (0.0)	0 (0.0)
	T5457C (D1819D)			TT	TC	CC
rs1805126	Case	30	28	11 (36.7)	8 (26.7)	11 (36.7)
	Control	80		8 (10.0)	52 (65.0)	20 (25.0)
	T5963G (L1988R)			TT	TG	GG
	Case	30	28	27 (90.0)	3 (10.0)	0 (0.0)
	Control	80		78 (97.5)	2 (2.5)	0 (0.0)

dbSNP ID: database single nucleotide polyporphysm

the reaction mixture was electrophoresed in a 2% agarose gel and stained with ethidium bromide (EtBr). Amplified PCR products were purified using the QIAquick PCR purification kit (Qiagen, Hilden, Germany), and directly sequenced using the BigDye Terminator Ver 3.1 cycle sequencing kit (Applied Biosystems, Foster city, CA, USA) and an ABI PRISM 3100 Genetic Analyzer (Applied Biosystems, Foster City, CA, USA). Sequencing results were compared with reference sequences (SCN5A/NM_198056.2/ENSG00000183873/ENST00000333535) using the alignment program BLAST 2.0 of the national center of biotechnology information (NCBI; Bethesda, MD, USA), and the portion of variation that occurred was determined.

Three-dimensional modeling of *SCN5A*

The structural model of the human *SCN5A* domain was obtained from the Automated SWISS-MODEL version 8.05 (Swiss Institute of Bioinformatics Biozentrum, Basel, Switzerland).[8-10] Superimposition, model building, construction of insertion regions, structure validation, and calculation of structural properties were carried out using the subprograms ProMod, SPDBV, Loop, LoopDB, Parameters, and Topologies, which are available in the Automated Swiss-Model Package Program (http://swissmodel.expasy.org). Pymol v0.99 and Cn3D (www. ncbi.nlm.nih.gov/Structure/CN3D/cn3d.html) were used to display the three-dimensional model structures.

Patch-clamp recording

Whole-cell configuration of the voltage-clamp technique was used as described elsewhere.[11] Briefly, whole-cell configuration was made in Tyrode's solution. Pipette resistances were 1.5–3 MΩ. After achieving a gigaseal, the test-pulse current was nulled by adjusting the pipette capacitance compensator with both fast and slow components. After break-in, the whole-cell charging transient was nulled by adjusting whole-cell capacitance and series resistance. Voltage control protocols were generated with an Axopatch 200B amplifier/Digidata 1440A acquisition system using the pCLAMP-10 software (Molecular Devices/Axon, Sunnyvale, CA, USA). Whole-cell recording was analyzed using Clampfit 10.2 (Axon, Sunnyvale, CA, USA). For measuring I_{Na}, we

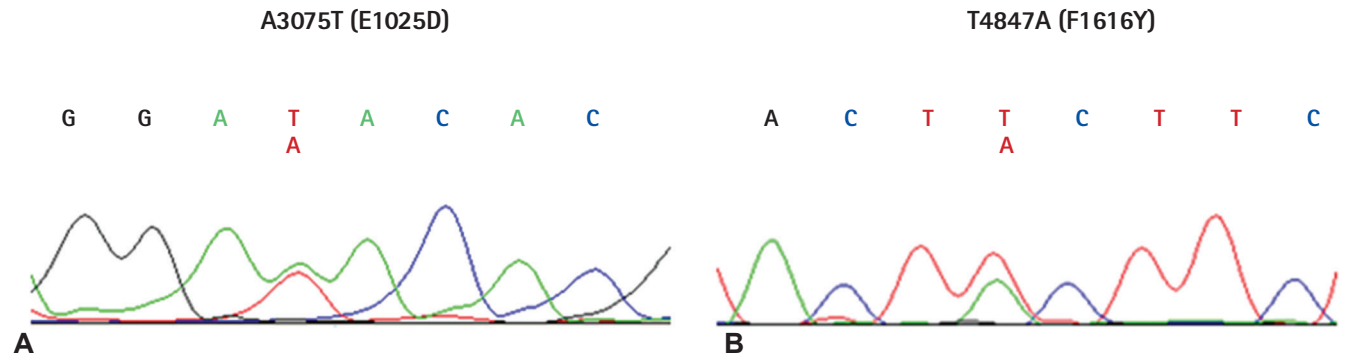

Fig. 1. DNA sequencing analysis results of the newly discovered *SCN5A* gene variants in this study. (A) DNA sequencing results of *SCN5A* exon 17. A3075T is a heterozygous nucleotide change, and causes an amino acid change from glutamine to aspartate. (B) DNA sequencing results of *SCN5A* exon 28. T4847A is a heterozygous nucleotide change, and causes an amino acid change from phenylalanine to tyrosine. All DNA sequence electropherograms show non-synonymous nucleotide changes in the sick sinus syndrome patients.

Fig. 2. Two variation sites (F1616Y and S1710L) within the 3D model of the *SCN5A* domain. F1616Y is located in the center of the second loop, which is well exposed, while the S1710L variation is located immediately following the 6th alpha helix.

used Tyrode's solution (see above) as the bath solution. The pipette solution contained (in mM) NaF 10, CsF 110, CsCl 20, EGTA 10, and HEPES 10 (pH 7.35 adjusted with CsOH). The HEK293 cells used in our experiments did not show significant persistent I_{Na} in the absence or presence of tetrodotoxin as previously described.[11)12)]

Results

Patient demographics

Table 2 shows patient demographics. The mean age is 56 years old, and the mean left ventricular ejection fraction was 65%. 9 patients were male. The mean sinus pause detected by surface ECG or Holter monitoring was 4.7 sec.

Gene sequencing

We sequenced all exons (exon 2-exon 28) of the *SCN5A* gene except for untranslated regions. Although we analyzed only 30 samples from Korean SSS patients, we identified 9 genetic variations, consisting of 2 synonymous, 6 non-synonymous, and 1 at the splicing donor site of the intron9-exon10 boundary (Table 3). Among these, 7 variations (G87A-A29A, IVS9-3C>A, A1673G-H558R, G3823A-D1275N, T5457C-D1819D, T5963G-L1988R, and C5129T-S1710L) have previously been reported in the American, Japanese, and Han Chinese populations, and their allele frequencies were similar to that in the Japanese or Chinese series. In addition, 2 novel variations (A3075T-E1025D and T4847A-F1616Y) were also found in two patients (Fig. 1). To compare with the control population, we analyzed normal samples using the same methods in order to determine whether the same variations existed in

 http://dx.doi.org/10.4070/kcj.2016.46.1.63

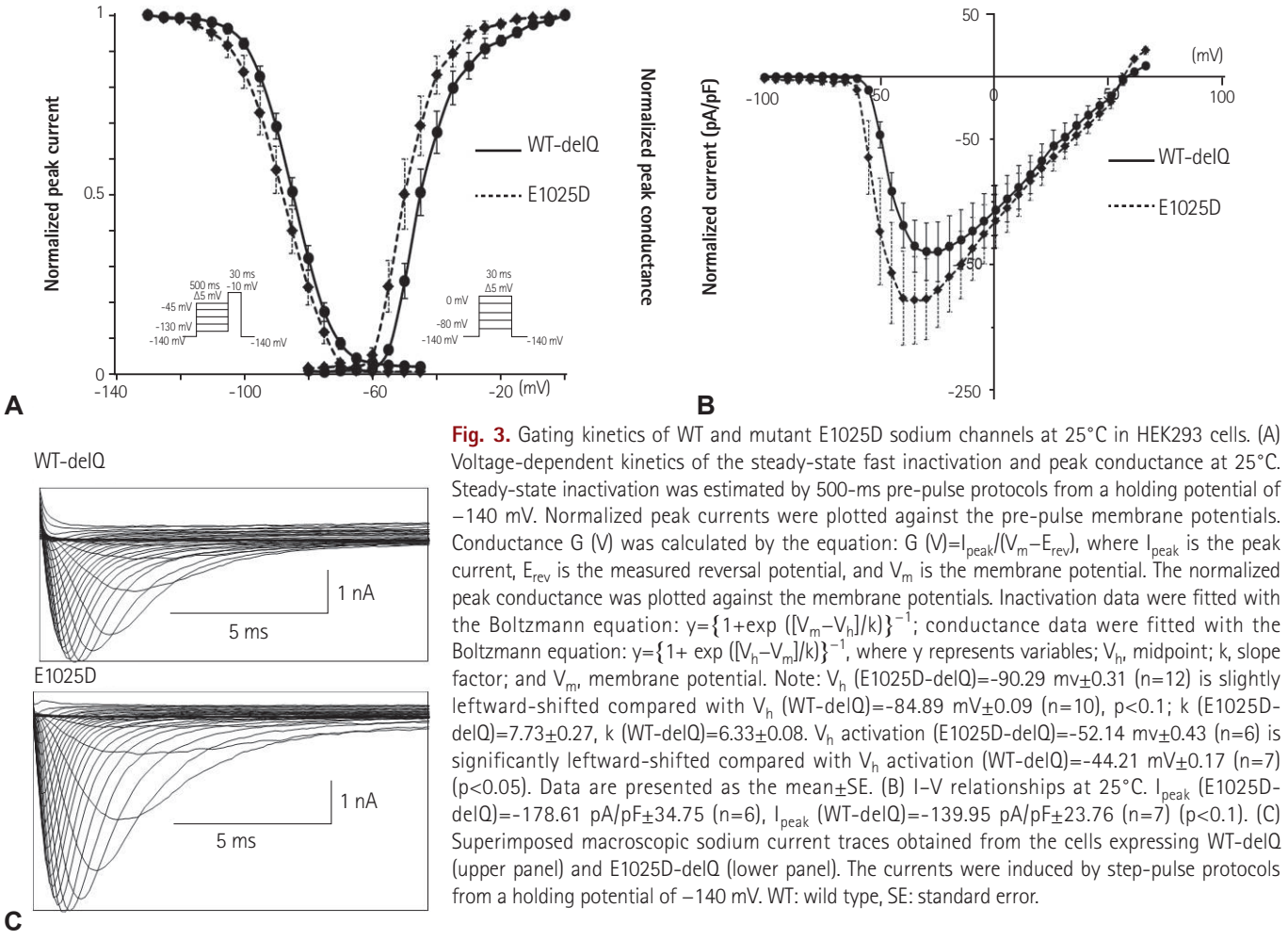

Fig. 3. Gating kinetics of WT and mutant E1025D sodium channels at 25°C in HEK293 cells. (A) Voltage-dependent kinetics of the steady-state fast inactivation and peak conductance at 25°C. Steady-state inactivation was estimated by 500-ms pre-pulse protocols from a holding potential of −140 mV. Normalized peak currents were plotted against the pre-pulse membrane potentials. Conductance G (V) was calculated by the equation: $G(V)=I_{peak}/(V_m-E_{rev})$, where I_{peak} is the peak current, E_{rev} is the measured reversal potential, and V_m is the membrane potential. The normalized peak conductance was plotted against the membrane potentials. Inactivation data were fitted with the Boltzmann equation: $y=\{1+\exp([V_m-V_h]/k)\}^{-1}$; conductance data were fitted with the Boltzmann equation: $y=\{1+\exp([V_h-V_m]/k)\}^{-1}$, where y represents variables; V_h, midpoint; k, slope factor; and V_m, membrane potential. Note: V_h (E1025D-delQ)=-90.29 mv±0.31 (n=12) is slightly leftward-shifted compared with V_h (WT-delQ)=-84.89 mV±0.09 (n=10), p<0.1; k (E1025D-delQ)=7.73±0.27, k (WT-delQ)=6.33±0.08. V_h activation (E1025D-delQ)=-52.14 mv±0.43 (n=6) is significantly leftward-shifted compared with V_h activation (WT-delQ)=-44.21 mV±0.17 (n=7) (p<0.05). Data are presented as the mean±SE. (B) I-V relationships at 25°C. I_{peak} (E1025D-delQ)=-178.61 pA/pF±34.75 (n=6), I_{peak} (WT-delQ)=-139.95 pA/pF±23.76 (n=7) (p<0.1). (C) Superimposed macroscopic sodium current traces obtained from the cells expressing WT-delQ (upper panel) and E1025D-delQ (lower panel). The currents were induced by step-pulse protocols from a holding potential of −140 mV. WT: wild type, SE: standard error.

their genes. Five variations (G87A-A29A, IVS9-3C>A, A1673G-H558R, T5963G-L1988R, and T5457C-D1819D) were also found in the control group, however the novel genetic variations (A3075T-E1025D and T4847A-F1616Y) were not present in any of the 80 normal controls.

Three-dimensional model of sinlge nucleotide polyporphysm

We successfully generated a three-dimensional model of the *SCN5A* domain (amino acid residues 1525-1750), which revealed 8 alpha-helices and 7 loops or kinks. We were able to use this model to analyze one of the novel variations (F1616Y) found in this study, and one of the known variations (S1710L) (Fig. 2). The location of the S1710L variation was immediately after the 6th alpha helix. The long 6th loop started from this area. In addition, the serine to leucine change likely generated an extended 6th alpha-helical structure. F1616Y was located in the center of the second loop, which is well exposed. Three-dimensional modeling of the other variations was not successful due to a lack of available crystal structures for the homologous templates.

Patch-clamp recording

Figs. 3 and 4 show the representative tracings and time course of I_{Na} at a frequency of 20/min. The I_{Na} was induced by a repetitive depolarization pulse (to −10 mV for 300 ms) from a holding potential of −140 mV. All experiments were carried out at room temperature. The peak I_{Na} and voltage-dependency in cells transfected with mutant E1025D were not significantly changed compared with wild-type (Fig. 3). However, the voltage-dependency of the Na^+ channel in mutant F1616Y-expressing HEK cells was significantly leftward-shifted compared with wild-type (V_h inactivation of F1616Y-delQ=-104.47 mV±0.21, n=7 vs. V_h inactivation of WT-delQ=-84.89 mV±0.09, n=12, p<0.005; V_h activation of F1616Y-delQ=-55.36 mv±0.22, n=8 vs. V_h activation of WT-delQ=-44.21 mV±0.17, n=7, p<0.005) (Fig. 4A). Furthermore, the peak I_{Na} in cells transfected with F1616Y demonstrated a 140% increase compared with wild-type (-335.13 pA/pF±24.04, n=8 vs -139.95 pA/pF±23.76, n=7, respectively, p<0.005) (Fig. 4B).

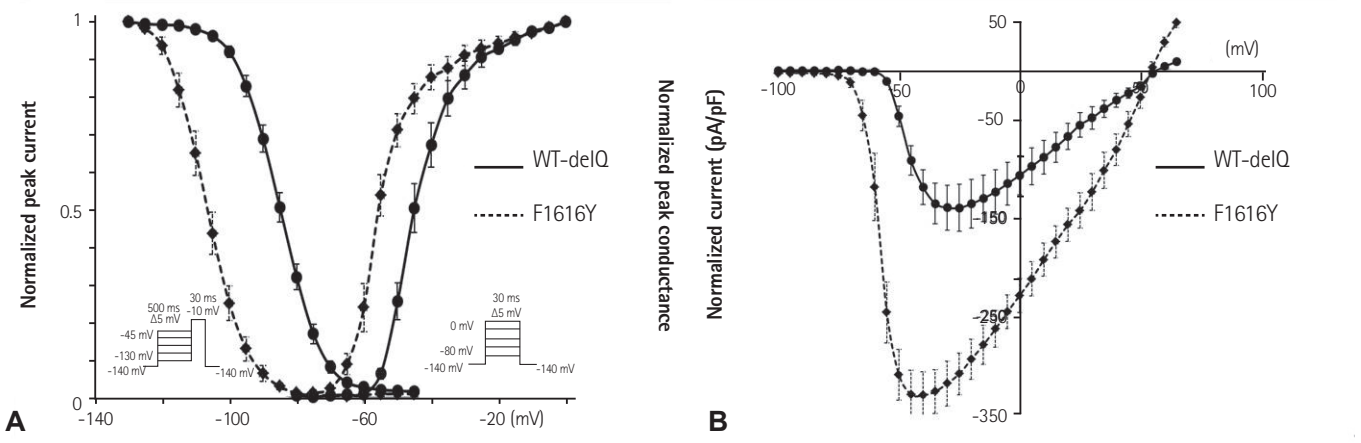

Fig. 4. Gating kinetics of WT and mutant F1616Y sodium channels at 25°C in HEK293 cells. (A) Voltage-dependent kinetics of the steady-state fast inactivation and peak conductance at 25°C. Steady-state inactivation was estimated by 500-ms pre-pulse protocols from a holding potential of −140 mV. Normalized peak currents were plotted against the pre-pulse membrane potentials. Conductance G (V) was calculated by the equation: $G(V)=I_{peak}/(V_m-E_{rev})$, where I_{peak} is the peak current, E_{rev} is the measured reversal potential, and V_m is the membrane potential. The normalized peak conductance was plotted against the membrane potentials. Inactivation data were fitted with the Boltzmann equation: $y=\{1+\exp([V_m-V_h]/k)\}^{-1}$; conductance data were fitted with the Boltzmann equation: $y=\{1+\exp([V_h-V_m]/k)\}^{-1}$, where y represents variables; V_h, midpoint; k, slope factor; and V_m, membrane potential. Note: V_h (F1616Y-delQ)=-104.47 mV±0.21 (n=8) is significantly leftward-shifted compared with V_h (WT-delQ)=-84.89 mV±0.09 (n=10), p<0.005; k (F1616Y-delQ)=6.52±0.18, k (WT-delQ)=6.33±0.08. V_h activation (F1616Y-delQ)=-55.36 mv±0.22 (n=8) is significantly leftward-shifted compared with V_h activation (WT-delQ)=-44.21 mV±0.17 (n=7), p<0.005). Data are presented as the mean±SE. (B) I-V relationships at 25°C. I_{peak} (F1616Y-delQ)=-335.13 pA/pF±24.04 (n=8), I_{peak} (WT-delQ)=-139.95 pA/pF±23.76 (n=7) (p<0.005). (C) Superimposed macroscopic sodium current traces obtained from the cells expressing WT-delQ (upper panel) and F1616Y-delQ (lower panel). The currents were induced by step-pulse protocols from a holding potential of −140 mV. WT: wild type, SE: standard error.

Discussion

In the present study, the genetic nucleotide sequence of *SCN5A* was determined in Korean SSS patients and compared with that of the controls. We found two novel genetic variations (A3075T-E1025D and T4847A-F1616Y). In addition, the normalized I_{Na} in mutant F1616Y-expressing HEK cells showed a leftward-shift in inactivation and activation, and the peak I_{Na} was increased.

The *SCN5A* gene consists of 28 exons and encodes a protein of 2016 amino acids, with a molecular mass of 227 kDa.[13] In our patients with SSS, there were 9 sites of nucleotide change from exon 2 to exon 28 of the *SCN5A* gene. Among these, 2 sites (G87A-A29A and IVS9-3C>A) have been reported as genetic variations in a Western study,[14] and T5457C-D1819D has already been reported as a variation or polymorphism without functional effects to the channel in Asian studies.[15-17] Recently, Gui et al.[18] reported that A1673G-H558R has variation-specific effects on *SCN5A*-related SSS. In addition, G3823A-D1275N, which is reported as a heterozygous loss-of-function variation, is related to reduced whole-cell currents due to impaired cell surface localization.[19]

Since a synonymous nucleotide change in the *SCN5A* gene is unlikely to induce a functional change in the Na^+ channel, a non-synonymous substitution was considered as a candidate for the variation associated with this disorder. The two new variations found in this study are non-synonymous and heterozygous changes. The variations may not affect the pathogenesis of SSS due to the opposite normal allele. Therefore, it is reasonable to suggest that the functional consequences of these changes should be assessed by measuring their effect on Na^+ channel activity, allowing assessment of a direct relationship between the variations and disease.

We can deduce the functional effect of the variations by structural simulations, which provide direction for subsequent studies. In the present study, we obtained some information from a structural model of *SCN5A* on the functional effect of the variations S1710L

http://dx.doi.org/10.4070/kcj.2016.46.1.63

and F1616Y. In the model, S1710L perturbs the Nav1.5 molecular structure from the 6th alpha helix – 6th loop structural changes. It is also likely that the physiological consequences of this model would be misfolding of the Nav1.5 protein.[20] However, F1616Y was located in the center of the second loop, which is well exposed. There is no significant steric hindrance or helix-packing problem with a change from phenylalanine to tyrosine at the 1616 site. Although there would be no significant structural changes with the F1616Y variation, one cannot exclude the possibility that it may be involved in protein-protein interactions, resulting in pathological consequences.

We used whole-cell configuration of the voltage-clamp technique to determine the effect of these genetic mutations. The mutation F1616Y led to a significant leftward-shift in the voltage-dependency of the Na^+ channel. Karin et al.[21] showed that some voltage-sensor Na^+ channel mutations can lead to a 10 mV leftward shift of the steady-state fast inactivation curve, which enhances inactivation. In their study, the heterologous expression of the two Na^+ channel mutations was shown to be important in pathogenesis by reducing the number of excitable channels. Similar to Lehmann-Horn's study,[21] the mutation F1616Y makes a leftward-shift in the Na^+ channel voltage-dependency, enhancing inactivation of the channel, and may be a cause of the pathogenesis of SSS, even in the heterologous mutation.

Most *SCN5A* mutations associated with sinus node dysfunction have shown a reduction in function or loss of function,[4] but rare *SCN5A* mutations such as L212P have been reported to have gain of function.[22] Mutations in *SCN5A* have been linked to LTQ3 due to an increase in persistent late I_{Na} (gain of function). However, the action potential in the sinoatrial node is largely calcium channel dependent.[23] One possible explanation for how gain of function mutations in *SCN5A* could lead to sinoatrial node dysfunction is due to failure of the impulses to propagate into the adjacent atrial myocardium. The large hyperpolarizing shift in activation of the F1616Y channel reduces the threshold potential for activation, leading to increased I_{Na}. The hyperpolarizing shift of steady-state inactivation and delayed recovery from inactivation reduce Na^+ channel availability and slow cardiac impulse conduction. Such opposing gating properties have been shown in the *SCN5A* mutation, G514C, responsible for isolated cardiac conduction disease.[24] The G514C channel exhibits a depolarizing shift in both activation and inactivation. It is assumed that the balance of opposing gating abnormalities as demonstrated in G514C, under the influence of additional factors involved in impulse propagation, may elicit exit block in the sinoatrial node. In LQT3 families with 1795insD mutations, a persistent inward current or a negative shift in inactivation has been shown to impair the coupling of electrical events between the pacemaker cells and those surrounding them within the sinoatrial node. This led to impaired propagation of electrical activity from the sinoatrial node to atrial tissue.[25]

In our study, the patients with novel genetic variations (A3075T-E1025D and T4847A-F1616Y) are all female and were diagnosed at a relative young age (<60 years), meaning that the genetic variation may be related to a clinical event. In particular, the patient with a genetic variation at T4847-F1616Y had a family history of SSS. Her mother had complained of SSS-related symptoms such as dizziness and palpitations in her forties. She was diagnosed by an electrophysiological study in her sixties. However, we could not confirm the presence of the genetic variation because she was already deceased. Therefore, we believe that this study on the functional consequences of the genetic variation is important.

A limitation of this study is the relatively small number of patients. In addition, we are not able to explain the exact relationship between the gain-of-function of F1616Y and SSS. However, Makita et al.[22] reported gain of function of *SCN5A* in one family with congenital atrial standstill similar to our study. Finally, *SCN5A* may play a role in the SA node,[4] therefore, we are planning to generate animal models for future research.

To our knowledge, this is the first study to determine a link between genetic variations in *SCN5A* and Korean patients with SSS. In this study, we demonstrated that there are 2 novel genetic variations (E1025D and F1616Y) in *SCN5A* in Korean patients with SSS.

Acknowledgments

The research was supported by the Ministry of Science, ICT and Future Planning Through the Development for IT·SW industrial convergence original technology (ID:R0101-15-0147, 2012).

We are grateful to Dr. Tomohiko Ai for his critical reading of the manuscript.

References

1. Mangrum JM, DiMarco JP. The evaluation and management of bradycardia. *N Engl J Med* 2000;342:703-9.
2. Benson DW, Wang DW, Dyment M, et al. Congenital sick sinus syndrome caused by recessive mutations in the cardiac sodium channel gene (SCN5A). *J Clin Invest* 2003;112:1019-28.
3. Groenewegen WA, Firouzi M, Bezzina CR, et al. A cardiac sodium channel mutation cosegregates with a rare connexin40 genotype in familial atrial standstill. *Circ Res* 2003;92:14-22.

4. Lei M, Zhang H, Grace AA, Huang CL. SCN5A and sinoatrial node pacemaker function. *Cardiovasc Res* 2007;74:356-65.
5. Schulze-Bahr E, Eckardt L, Breithardt G, et al. Sodium channel gene (SCN5A) mutations in 44 index patients with Brugada syndrome: Different incidences in familial and sporadic disease. *Hum Mutat* 2003;21:651-2.
6. Tan HL, Bezzina CR, Smits JP, Verkerk AO, Wilde AA. Genetic control of sodium channel function. *Cardiovasc Res* 2003;57:961–73.
7. Shin CH, Kim NH, Kim KH, et al. A family with a missense mutation in the SCN5A gene. *Korean Circ J* 2003;33:150-4.
8. Arnold K, Bordoli L, Kopp J, Schwede T. The SWISS-MODEL workspace: a web-based environment for protein structure homology modelling. *Bioinformatics* 2006;22:195-201.
9. Kiefer F, Arnold K, Künzli M, Bordoli L, Schwede T. The SWISS-MODEL Repository and associated resources. *Nucleic Acids Res* 2009;37(Database issue):D387-92.
10. Schwede T, Kopp J, Guex N, Peitsch MC. SWISS-MODEL: an automated protein homology-modeling server. *Nucleic Acids Res* 2003;31:3381-5.
11. Turker I, Yu CC, Chang PC, et al. Amiodarone inhibits apamin-sensitive potassium currents. *PLoS One* 2013;8:e70450.
12. Xi Y, Ai T, De Lange E, et al. Loss of function of hNav1.5 by a ZASP1 mutation associated with intraventricular conduction disturbances in left ventricular noncompaction. *Circ Arrhythm Electrophysiol* 2012;5:1017-26.
13. Gellens ME, George AL Jr, Chen LQ, et al. Primary structure and functional expression of the human cardiac tetrodotoxin-insensitive voltage-dependent sodium channel. *Proc Natl Acad Sci U S A* 1992;89:554-8.
14. Lehtinen AB, Daniel KR, Shah SA, et al. Relationship between genetic variants in myocardial sodium and potassium channel genes and QT interval duration in diabetics: The Diabetes Heart Study. *Ann Noninvasive Electrocardiol* 2009;14:72–9.
15. Chen JZ, Xie XD, Wang XX, Tao M, Shang YP, Guo XG. Single nucleotide polymorphisms of the SCN5A gene in Han Chinese and their relation with Brugada syndrome. *Chin Med J (Engl)* 2004;117:652-6.
16. Shin DJ, Jang Y, Park HY, et al. Genetic analysis of the cardiac sodium channel gene SCN5A in Koreans with Brugada syndrome. *J Hum Genet* 2004;49:573-8.
17. Takahata T, Yasui-Furukori N, Sasaki S, et al. Nucleotide changes in the translated region of SCN5A from Japanese patients with Brugada syndrome and control subjects. *Life Sci* 2003;72:2391-9.
18. Gui J, Wang T, Trump D, Zimmer T, Lei M. Mutation-specific effects of polymorphism H558R in SCN5A-related sick sinus syndrome. *J Cardiovasc Electrophysiol* 2010;21:564-73.
19. Gui J, Wang T, Jones RP, Trump D, Zimmer T, Lei M. Multiple loss-of-function mechanisms contribute to SCN5A-related familial sick sinus syndrome. *PLoS One* 2010;5:e10985.
20. Cha K, Reeves PJ, Khorana HG. Structure and function in rhodopsin: destabilization of rhodopsin by the binding of an antibody at the N-terminal segment provides support for involvement of the latter in an intradiscal tertiary structure. *Proc Natl Acad Sci U S A* 2000;97:3016-21.
21. Jurkat-Rott K, Mitrovic N, Hang C, et al. Voltage-sensor sodium channel mutations cause hypokalemic periodic paralysis type 2 by enhanced inactivation and reduced current. *Proc Natl Acad Sci U S A* 2000;97:9549-54.
22. Makita N, Sasaki K, Groenewegen WA, et al. Congenital atrial standstill associated with coinheritance of a novel SCN5A mutation and connexin 40 polymorphisms. *Heart Rhythm* 2005;2:1128-34.
23. Baruscotti M, DiFrancesco D, Robinson RB. A TTX-sensitive inward sodium current contributes to spontaneous activity in newborn rabbit sino-atrial node cells. *J Physiol* 1996;492(Pt 1):21–30.
24. Tan HL, Bink-Boelkens MT, Bezzina CR, et al. A sodium-channel mutation causes isolated cardiac conduction disease. *Nature* 2001;409:1043–7.
25. Veldkamp MW, Wilders R, Baartscheer A, Zegers JG, Bezzina CR, Wilde AA. Contribution of sodium channel mutations to bradycardia and sinus node dysfunction in LQT3 families. *Circ Res* 2003;92:976-83.

 http://dx.doi.org/10.4070/kcj.2016.46.1.63